

Far-infrared magnetospectroscopy of the Landau-level structure in graphite

R. E. Doezema, W. R. Datars,* and H. Schaber

Physik Department, Technische Universität München, 8046 Garching, Germany

A. Van Schyndel

Department of Physics, McMaster University, Hamilton, Ontario L8S 4M1, Canada

(Received 26 December 1978)

We present a study of the magnetorefectivity of pyrolytic graphite in fields up to 8 T. Circularly polarized radiation at fixed laser frequencies in the energy range 3–16 meV was used. In addition to the usual intraband (cyclotron resonance) transitions, we observe transitions from the special central and leg electron levels first predicted by Dresselhaus. The field positions of the resonances are compared to those resulting from the detailed theoretical calculation of Nakao. Excellent agreement is obtained for the value of the trigonal warping parameter γ_3 equal to 0.315 ± 0.015 eV.

I. INTRODUCTION

Although the band structure of graphite has been well established experimentally¹ within the framework of the Slonczewski-Weiss model,² certain questions remain regarding the magnitude and influence of the trigonal warping. We present here a study of the magnetorefectivity of pyrolytic graphite in a frequency and magnetic field range where the trigonal warping is of particular importance in understanding the experimental results.

The Fermi surface of graphite consists of electron and hole pockets along the *HKH* edges of the hexagonal Brillouin zone (Fig. 1). At a given edge the electron pocket is centered about *K* with adjacent hole pockets extended on either side towards the *H* points. In the experiment we employ the Faraday geometry with the magnetic field along the *HKH* edge, i.e., along the \vec{c} axis. Most of the resonance structure observed is due to electron orbits centered at *K* where the effect of the trigonal warping is strongest. At the Fermi energy, the effect of the trigonal warping, whose strength is denoted by the parameter γ_3 , is to deform the Fermi surface from a surface with a circular cross section ($\gamma_3=0$) to the warped surface evident in Fig. 1. The velocity component perpendicular to the magnetic field direction contains harmonics *l* consistent with the trigonal symmetry, leading to the selection rule for cyclotron resonance,

$$\omega = (3N+1)\omega_c, \quad N=0, \pm 1, \pm 2, \dots, \quad (1)$$

Here ω is the excitation frequency and ω_c is the cyclotron frequency.

For circularly polarized radiation, one finds for the electron-active mode (the polarization sense which excites cyclotron resonance for circular electron orbits) the allowed harmonics $l = 1, 4, 7, \dots$

of the cyclotron frequency. Similarly for the hole-active mode, the harmonics $l = 2, 5, 8, \dots$ are found. The absorption strengths of the various harmonics are related to the degree of trigonal warping, i.e., to γ_3 . This was exploited by Ushio *et al.*,³ who analyzed the microwave cyclotron resonance experiment of Suematsu and Tanuma⁴ to obtain $\gamma_3 = 0.21 \pm 0.02$ eV. Their value is rather lower than the value 0.29 ± 0.02 eV found by Schroeder *et al.*⁵ from an analysis of interband magneto-optical absorption strengths.

Dresselhaus⁶ was the first to point out that the

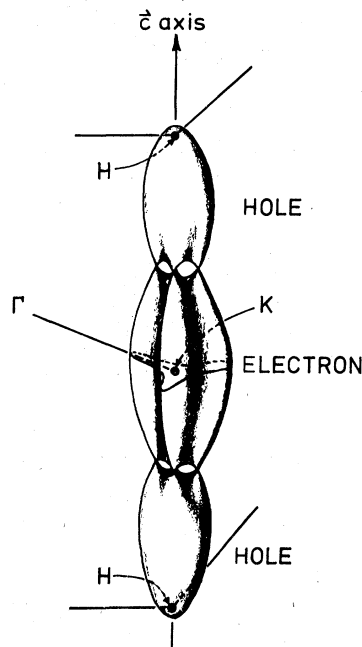


FIG. 1. Fermi surface of graphite.

existence of local extrema in the band dispersion normal to the \tilde{c} axis, which are due to γ_3 , leads to new types of Landau levels deep below the Fermi energy [Fig. 2(a)]. Using semiclassical Bohr-Sommerfeld quantization, he found orbits centered on K (central orbits) and a threefold degenerate set of orbits displaced away from K (leg orbits) as depicted in Fig. 2(b). Since these levels owe their existence to a finite γ_3 , a spectroscopic study of transitions from such levels should be a sensitive probe of the value of γ_3 .

The first spectroscopic evidence for these levels was given by Platts *et al.*,⁷ who used Fourier interferometric techniques. They studied the magnetoreflexion at a variety of constant magnetic fields as a function of photon energy in the range

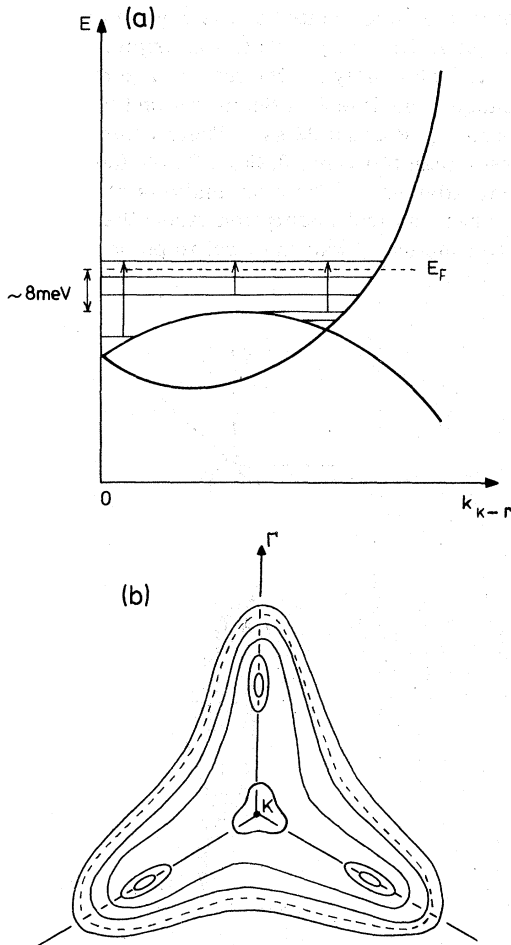


FIG. 2. Effect of trigonal warping on the energy dispersion near the K -point. (a) Schematic Landau levels with transitions from central and leg levels and from ordinary levels. The dispersion is shown along the axis from K to Γ . (b) Corresponding orbits in k space.

6–45 meV. Full details of this experiment are contained in a thesis.⁸

Since the new levels are located ~ 10 meV below the Fermi energy, it is desirable to carefully examine the magnetoreflexion near this energy. Here we present new and more detailed data at fixed laser frequencies in the range 3–16 meV using circular polarization. In interpreting our results we rely on the theoretical calculation of Nakao.⁹ His calculation, although incorporating the new Dresselhaus orbits, treats the magnetic-energy-level structure more accurately than the semiclassical Bohr-Sommerfeld calculation.

II. EXPERIMENTAL RESULTS

Before describing our results, we briefly relate the main features of the experimental system.

Far-infrared radiation was provided by a cw gas laser operated at four selected wavelengths: 336.6 μm (3.68 meV), 118.6 μm (10.45 meV), 84.3 μm (14.70 meV), and 78.5 μm (15.80 meV). The sample (a 7×10 -mm² piece of pyrolytic graphite with thickness ~ 1 mm) was mounted in a polarizer unit located within a superconducting magnet capable of providing fields up to ~ 8 T, directed normal to the sample surface. All measurements were performed at 4.2 K. The circular-polarizer reflectometer¹⁰ is an arrangement of a linear polarizer and a quarter-wave plate whose thickness was chosen appropriately for each wavelength. The degree of circular polarization was best at 119 μm : the unwanted mode was seen at the detector (a Ga-doped Ge bolometer) with only $\sim 2\%$ of the intensity of the wanted mode. For the other frequencies this percentage was higher, on the order of 10%, and evidence of "cross talk" can be seen in the experimental curves.

To demonstrate the size of the changes in sample reflectivity R induced by cyclotron resonance, we show in Fig. 3 experimental traces of R versus magnetic field in both polarization modes. Such curves are obtained by chopping the laser beam and dividing the phase-detected bolometer signal by the signal from a second detector proportional to the beam intensity. To avoid drift problems and to enhance the structure in such curves, it is highly advantageous to modulate the magnetic field (in our case at ~ 20 Hz) and detect the derivative dR/dH . Let us consider first the results at the lowest of our frequencies with wavelength $\lambda = 337$ μm .

In Fig. 4 the observed dR/dH spectra are shown for both polarization modes at 337 μm . These spectra resemble those at microwave frequencies,⁴ exhibiting the indicated subharmonic structure expected for a trigonally warped Fermi surface.

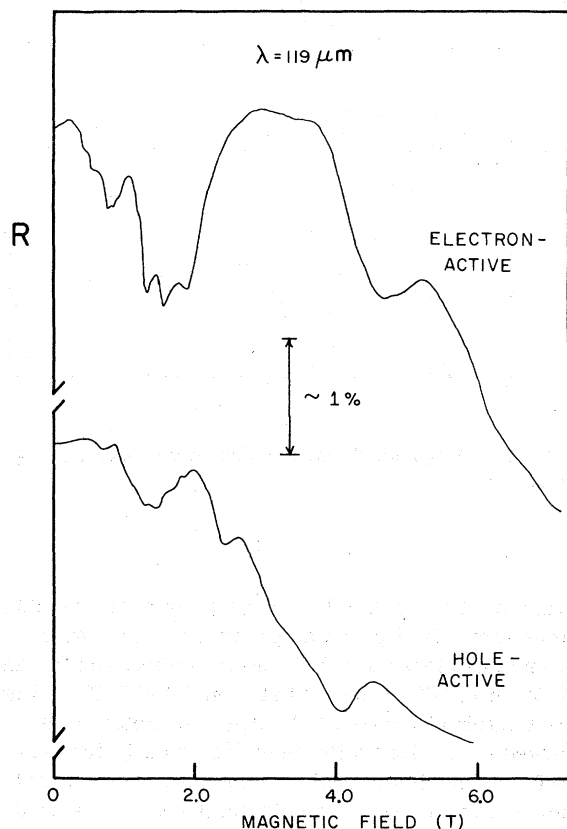


FIG. 3. Magnetorelectance of pyrolytic graphite at $119 \mu\text{m}$. The traces are taken in the Faraday geometry at 4.2 K with the magnetic field along the \bar{c} axis.

Even though the photon energy (3.68 meV) is not high enough to probe the central and leg levels, nonparabolicity does affect the resonance fields. Thus the resonances should not be directly inter-

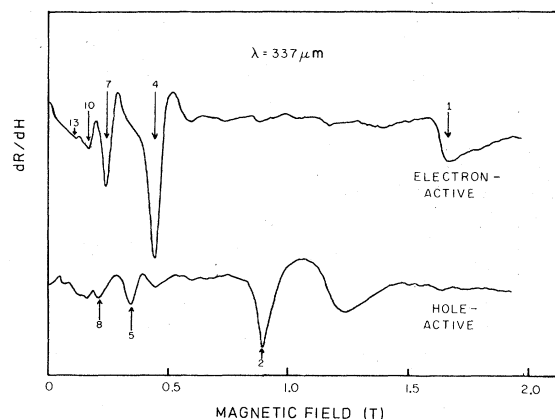


FIG. 4. Magnetorelectance derivative spectra at $337 \mu\text{m}$. Peaks are labeled by harmonic number.

preted in terms of an effective mass. Since we have not determined the dielectric function and thus the line shape, it is not clear exactly where the resonances are to be marked. Judging from the line-shape calculations (at far higher photon energies) of Schroeder *et al.*,⁵ the field values at the minima in dR/dH should correspond closely to the resonance fields. For convenience we adopt this criterion in determining the resonance positions. We note, however, that at microwave frequencies, the fields at the maximum positive slope in dR/dH were found to correspond to the resonance condition. We take this possible spread in field values into account when comparing to the theoretically predicted transitions.

The dramatic changes in the resonance spectra at photon energies high enough to probe the low-lying Landau levels are immediately apparent in Figs. 5–7. At $119 \mu\text{m}$ classical subharmonic features can still be recognized, as indicated in Fig. 5, but these are broken up into individual resonance peaks. This distinctively quantum aspect is even more enhanced at $84 \mu\text{m}$ (Fig. 7). As suggested in the figures, we are able to identify the individual resonances with reference to the calculation described in Sec. III.

III. COMPARISON WITH NAKAO'S CALCULATION

The Slonczewski-Weiss Hamiltonian,² which describes the graphite band structure along the HKH Brillouin-zone edge, is a 4×4 matrix containing seven parameters: $\gamma_0, \gamma_1, \gamma_2, \gamma_3, \gamma_4, \gamma_5$, and Δ . Their values are determined experimentally—chiefly by the de Haas-van Alphen effect, cyclotron resonance, and by magneto-optical interband spectroscopy. Calculating the Landau-level struc-

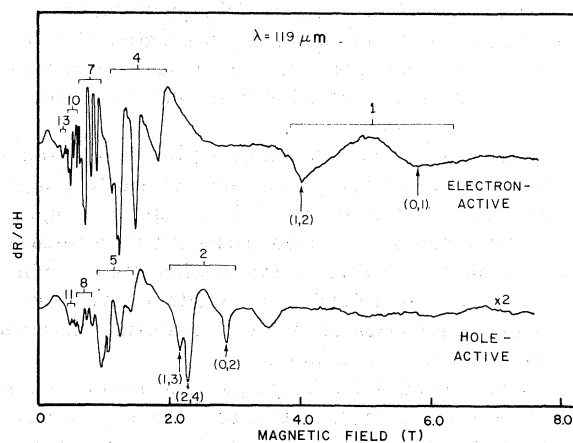


FIG. 5. Magnetorelectance derivative spectra at $119 \mu\text{m}$. Bracketed ranges are labeled by harmonic number.

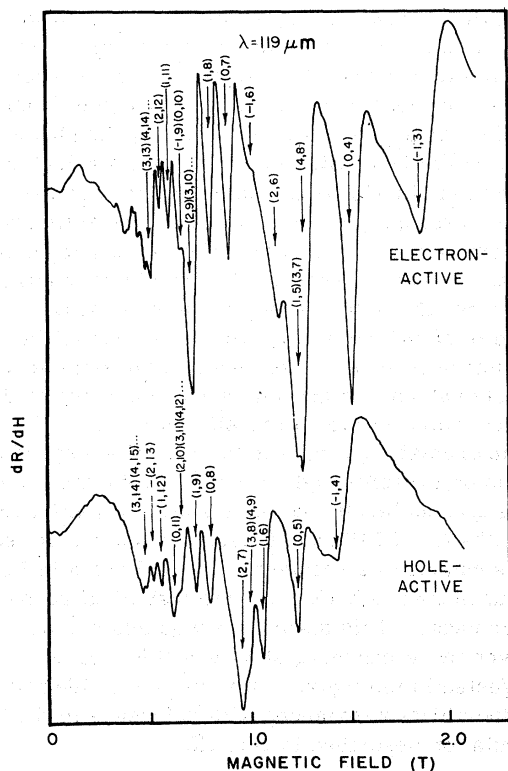


FIG. 6. Low-field detail of the 119- μm derivative spectra.

ture with trigonal warping presents considerable difficulty since the Hamiltonian matrix in the presence of a magnetic field is infinite for $\gamma_3 \neq 0$, and a perturbation expansion is not suitable⁵ for the range of values ($\gamma_3 \geq 0.2$ eV) required experimentally.

Dresselhaus⁶ avoided this problem by use of semiclassical Bohr-Sommerfeld quantization. With this treatment, however, discontinuities in the level structure occur at the crossover energy between leg and central behavior and the more usual level behavior.

These discontinuities are nonexistent in Nakao's calculation⁹: the special leg and central levels go smoothly over into the usual levels as the magnetic field increases. Nakao treats the infinite-matrix problem by grouping the original Hamiltonian into three submatrices which are then truncated. The diagonalization of the large resulting matrices is performed by computer.

We have used Nakao's computer program to predict the Landau-level structure at the K point for magnetic fields between 0.3 and 9.0 T. The band parameters were those used by Nakao⁹ except for γ_3 , which was allowed to take on a sequence of

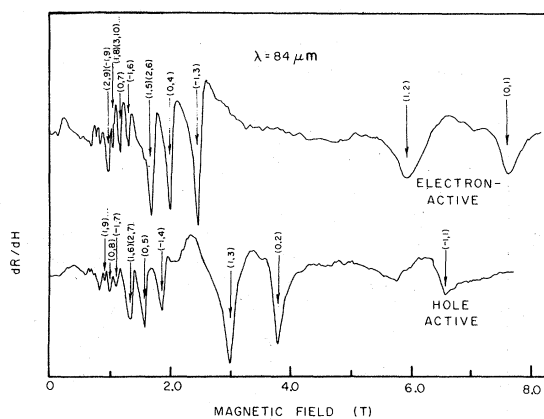


FIG. 7. Magnetorelectance derivative spectra at 84 μm .

values. For each value of γ_3 , a fan chart such as that shown in Fig. 8 was produced. (The levels were calculated at 0.1-T intervals between 0.3 and 2 T, at 0.2-T intervals between 2 and 3 T, and at 1-T interval above 3 T.) Magnetic fields of allowed transitions with energies equal to the far-infrared photon energies were read off the chart and compared with experimental resonance fields.

Which transitions are allowed is easily determined with Nakao's classification scheme. As in Fig. 8, every magnetic level is labeled by a letter a , b , or c , referring to matrix group or wavefunction mixture, and by a quantum number n .⁹ In the electron-active mode of circular polarization, transitions $a \rightarrow b$, $b \rightarrow c$, and $c \rightarrow a$ are allowed. In

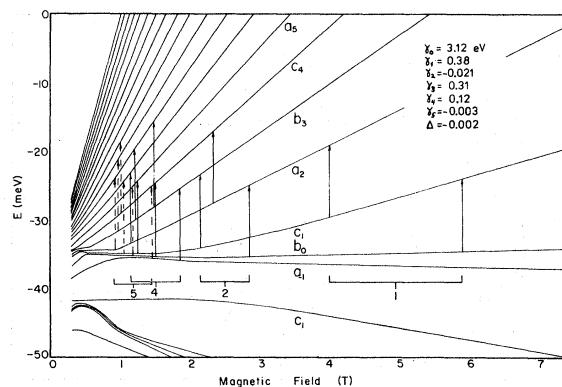


FIG. 8. Nakao's Landau-level structure. Transitions corresponding to $\lambda = 119 \mu\text{m}$ are indicated; bracketed ranges are labeled by harmonic number.

the hole-active mode the allowed transitions are $a \rightarrow c$, $c \rightarrow b$, and $b \rightarrow a$. With reference to the change l in quantum number n , these rules are equivalent to the condition expressed in Eq. (1). In our energy range, where we are considering only intraband transitions, we can unambiguously label the transition from level m to level n as (m, n) without reference to the letter classification. Thus we have using Eq. (1): $l = n - m = |3N + 1|$.

Nakao has stated⁹ the matrix sizes necessary to achieve convergence within 0.1 meV. We have deviated slightly from these sizes and have used the dimensions 100×100 in the field range 0.3–1.0 T and 60×60 for fields above 1.0 T. At the crossover field, 1.0 T, the results at the K point for either dimension agree to within 0.1 meV. Except for the lowest fields, ≈ 0.5 T, we therefore expect the calculation to be accurate to within 1% for the wavelengths 119, 84, and 78 μm , and to within 3% for 337 μm . For the three shorter wavelengths the expected error in the calculated results is less than the uncertainty in determining the experimental peak positions ($\sim 1.5\%$) and certainly less than the uncertainty ($\sim 3\%$) in marking the resonance point on the experimental line shape.

To determine the value of γ_3 , we choose to fit certain prominent resonances (indicated in Table I) whose positions are particularly sensitive to γ_3 and which are found in the field range 1–2.5 T. For each transition i we compare the theoretical resonance position H_i^T with the experimentally determined position H_i^E , and form the average relative deviation in percent:

$$\alpha = \frac{1}{M} \sum_{i=1}^M \left(\frac{H_i^E - H_i^T}{H_i^E} \right) \times 100\%. \quad (2)$$

The results are shown in Fig. 9, where we plot α vs γ_3 for 119 and 78 μm . With M in Eq. (2) equal to 6 or 7, we estimate from the above discussion concerning uncertainties that the error limits on α are about $\pm 1.5\%$. Using our dR/dH minimum criterion for the resonance position H_i^E , we find then from the lines labeled " dR/dH " in Fig. 9, $\gamma_3 = 0.31 \pm 0.01$ eV. If we use the criterion of Ref. 4, marking the position H_i^E at the maximum positive slope of the dR/dH peaks—this corresponds roughly to marking the dips in the $R(H)$ curves—we arrive at the lines labeled " $R(H)$ " in Fig. 9 and at the subsequent γ_3 value 0.323 ± 0.010 eV. If we include the line-shape uncertainty, therefore, we obtain the value $\gamma_3 = 0.315 \pm 0.015$ eV. The root-mean-square deviations at the optimal γ_3 values are all about 1% and minimal.

The values of the other band parameters are shown in Fig. 8. They are essentially those given by Dresselhaus⁶ and, except for the values of γ_5

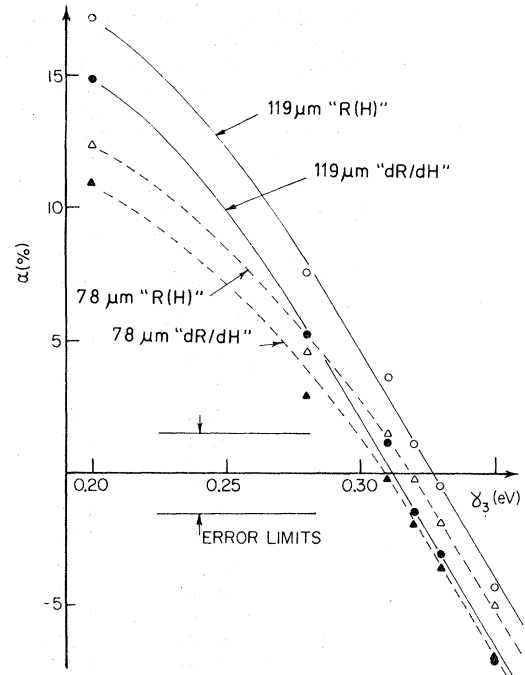


FIG. 9. Average relative deviation of calculated from observed resonance positions vs. γ_3 . Both ways of marking the observed positions (dR/dH and $R(H)$) are indicated for each frequency.

and Δ , are nearly identical with those given more recently by Dresselhaus *et al.*¹¹ To test the dependence of our γ_3 value on the values of the other parameters, we have used the older and somewhat different set of parameters given by Schroeder *et al.*⁵ Again we obtain the value for γ_3 given above.

In Table I we list the experimentally determined dR/dH minimum positions at 119, 84, and 78 μm , and compare these to the calculated resonance fields for $\gamma_3 = 0.31$ eV. As is easily verified, the agreement is excellent.

A final point in this section concerns the 337- μm data of Fig. 4. Similar results, obtained with unpolarized radiation, were found by Robinson.¹² Above 0.3 T, the calculation with $\gamma_3 = 0.31$ eV predicts a first harmonic, $l=1$, resonance at 1.70 T due to a (3, 4) transition. We mark the dR/dH minimum at 1.67 T. The second, fourth, and fifth harmonics arise from multiple transitions. The resonance fields lie sufficiently close so that for each harmonic, a single peak is to be expected whose linewidth depends significantly on the spread in resonance fields. The average fields for $l=2, 4$, and 5, respectively, are predicted as 0.92, 0.47, and 0.375 T. The dR/dH minima are at 0.89, 0.45, and 0.35 T. As we noted above, the accuracy

TABLE I. Comparison of calculated and observed resonance fields at three far-infrared frequencies. The values are tabulated up to the eighth harmonic (l) and the transitions are labeled by initial and final Landau level. The experimental resonance positions are marked at the dR/dH minima with maximum certainty 1.5%. The calculated values, accurate to better than 1%, are from the Nakao model with $\gamma_3=0.31$ eV.

l	Transition	Resonance fields (T)					
		119 μm		84 μm		78 μm	
		calc.	obs.	calc.	obs.	calc.	obs.
1	(0,1)	5.85	5.82	7.61	7.49	8.06	...
	(1,2)	4.02	4.02	5.96	5.86	6.50	6.45
	(-1,1)	6.54	6.56	6.92	6.91
2	(0,2)	2.85	2.91	3.75	3.78	3.98	4.01
	(1,3)	2.13	2.20	2.99	2.99	3.22	3.20
	(2,4)	2.29	2.33
	(-1,3)	1.84	1.86 ^a	2.44	2.46	2.60	2.58 ^a
4	(0,4)	1.47	1.51 ^a	1.95	1.96	2.06	2.09 ^a
	(1,5)	1.24	1.24 ^a	1.64	1.67	1.75	1.77
	(2,6)	1.16	1.145	1.68	1.67	1.81	1.82
	(3,7)	1.25	1.265	1.76	1.67 ^b
	(4,8)	1.27	1.265
	(-1,4)	1.43	1.42 ^a	1.89	1.86	2.005	1.99 ^a
	(0,5)	1.20	1.23 ^a	1.58	1.57	1.68	1.69 ^a
	(1,6)	1.045	1.06 ^a	1.37	1.35	1.46	1.45
5	(2,7)	0.946	0.95	1.35	1.35	1.46	1.45
	(3,8)	1.005	0.99	1.42	1.35 ^b	1.53	1.45 ^b
	(4,9)	1.015	0.99
	(5,10)	1.025	0.99
	(-1,6)	1.01	1.00	1.31	1.31	1.40	1.38 ^a
	(0,7)	0.898	0.90	1.165	1.17	1.24	1.24 ^a
7	(1,8)	0.795	0.805	1.04	1.05	1.11	1.11 ^a
	(2,9)	0.721	0.72	0.975	0.97	1.05	1.03
	(3,10)	0.730	0.72	1.01	1.05	1.08	1.045
	(4,11)	0.750	0.72	1.035	1.05	1.11	1.11
	(5,12)	0.754	0.72	1.033	1.05	1.11	1.11

	(-1,7)	1.145	1.11	1.22	1.20
	(0,8)	0.797	0.80	1.023	1.02	1.09	1.095
8	(1,9)	0.716	0.73	0.934	0.92	0.992	0.99
	(2,10)	0.650	0.645	0.865	0.84	0.925	0.91
	(3,11)	0.644	0.645	0.892	0.92	0.959	0.99
	(4,12)	0.664	0.645	0.907	0.92	0.970	0.99
	(5,13)	0.668	0.645	0.910	0.92	0.974	0.99

^aTransition used to fix value of γ_3 .

^bIdentification uncertain.

of the calculation is expected to be lower at 337 μm than at the other wavelengths, and furthermore to be deteriorating in the 0.3–0.5-T range. Alternatively, a change in parameters other than γ_3 could improve the agreement at 337 μm .

IV. DISCUSSION

We have shown that the resonances observed in the far-infrared magnetorefectivity are excellently accounted for by the Landau-level structure at

the K point predicted by Dresselhaus and calculated in detail by Nakao. The value for γ_3 which we have found (0.315 ± 0.015 eV) is consistent with that found by Schroeder *et al.*⁵ (0.29 ± 0.02 eV). The value for γ_3 obtained in the analysis of Ushio *et al.*³ (0.21 ± 0.02 eV) is inconsistent with our results, as seen in Fig. 9.

In our analysis we have assumed the resonance fields to be representative of the K -point Landau-level spacing, thus neglecting contributions to the resonance line shape due to transitions away from

K , along the \vec{c} axis (the " k_H " direction). Nakao⁹ has calculated the k_H dependence of the Landau levels at 1.0 T. The transition frequencies increase away from K , so the resonance fields at fixed frequency decrease. Thus the field values applicable for the K point must be marked higher in the resulting line shape. We expect, however, that as is usually the case in practice, the line shape is weighted in favor of those points where the transition frequency is extremal—the K point in this instance—and that the shift in peak position is at most $\sim 1\%$ (a fraction of the linewidth). Our neglect of k_H effects on peak positions is therefore surely justified.

In addition to providing a value for γ_3 , our experiment can give a value for the Fermi energy E_F (with reference to the band-structure model). It can be determined from the Nakao calculation by the requirement that the initial state must be occupied and the final state unoccupied for a transition to be observable. Together with the model parameters given in Fig. 8, our experiment requires $-27 \text{ meV} < E_F < -25 \text{ meV}$ for transitions at fields less than 2 T where quantum effects are not expected¹³ to vary the Fermi energy significantly. A second determination of E_F is made from Nakao's model by determining the de Haas-van Alphen (dHvA) frequency from the magnetic field positions where the Landau levels cross a given energy. The energy corresponding to the dHvA frequency of $6.34 \pm 0.04 \text{ T}$, measured in a sample from the material used in our far-infrared work, is $-25.1 \pm 0.1 \text{ meV}$. (This dHvA frequency falls in the center of the range of previously reported values.¹⁴) Thus the dHvA value for E_F and that deduced from our far-infrared spectra are consistent within the model.

At high fields it is interesting to note the obser-

vation of quantum effects on E_F . Were the Fermi energy to remain constant as a function of magnetic field, the (1,2) transition at 84 and 78 μm would not be observable. That this transition is clearly present at both frequencies indicates that at $\sim 6.5 \text{ T}$ E_F has risen from its zero-field value of $\sim -25 \text{ meV}$ to $\sim -21 \text{ meV}$, in reasonable agreement with the prediction of Sugihara and Ono.¹³

A final point remains to be mentioned. All dR/dH peaks seen in our experiment can be identified with K -point resonances using the Nakao calculation, with the exception of a single peak at each frequency. This peak is seen in the hole-active mode at each frequency with the cyclotron mass $m_c = 0.039m_0$ at 337 μm , $0.040m_0$ at 119 μm , $0.045m_0$ at 84 μm , and $0.044m_0$ at 78 μm (m_0 is the free-electron mass). It appears to be the same as the peak observed in the hole-active mode at microwave frequencies and labeled X by Suematsu and Tanuma.⁴ The cyclotron mass values correspond closely with the majority-hole mass seen in the dHvA effect.¹ However, it is not clear whether the peak is due to a hole resonance because the calculated hole cyclotron mass shows no corresponding extremum as a function of k_H .^{3,9}

ACKNOWLEDGMENTS

We express our gratitude to K. Nakao for allowing us to use his computer program in calculating the Landau-level structure. We are grateful to Z. Altounian for measuring the dHvA frequency. For helpful communication and discussion we wish to thank G. Dresselhaus, M. S. Dresselhaus, H. D. Drew, and B. Vinter. One of us (W.R.D.) thanks F. Koch for the hospitality of his group at the TU München.

*Permanent address: Dept. of Physics, McMaster Univ., Hamilton, Ontario, L8S 4M1, Canada.

¹For reviews and further references see J. W. McClure, in *Proceedings of the Conference on the Physics of Semimetals and Narrow-Gap Semiconductors, 1970* edited by D. L. Carter and R. T. Bate (Pergamon, New York, 1971), p. 127; I. L. Spain, *Phys. Chem. Carbon* **8**, 1 (1973).

²J. C. Slonczewski and P. R. Weiss, *Phys. Rev.* **109**, 272 (1958).

³H. Ushio, T. Uda, and Y. Uemura, *J. Phys. Soc. Jpn.* **33**, 1551 (1972).

⁴H. Suematsu and S. Tanuma, *J. Phys. Soc. Jpn.* **33**, 1619 (1972).

⁵P. R. Schroeder, M. S. Dresselhaus, and A. Javan, in *Proceedings of the Conference on the Physics of Semimetals and Narrow-Gap Semiconductors, 1970*, edited

by D. L. Carter and R. T. Bate (Pergamon, New York, 1971), p. 139.

⁶G. Dresselhaus, *Phys. Rev. B* **10**, 3602 (1974).

⁷D. A. Platts, D. D. L. Chung, and M. S. Dresselhaus, *Phys. Rev. B* **15**, 1087 (1977).

⁸D. A. Platts, Ph.D. thesis (MIT, 1975) (unpublished).

⁹K. Nakao, *J. Phys. Soc. Jpn.* **40**, 761 (1976).

¹⁰H. Schaber and R. E. Doezema, *Infrared Phys.* **18**, 247 (1978).

¹¹M. S. Dresselhaus, G. Dresselhaus, and J. E. Fischer, *Phys. Rev. B* **15**, 3180 (1977).

¹²A. K. V. Robinson, Masters thesis (Univ. of Maryland, 1974) (unpublished).

¹³K. Sugihara and S. Ono, *J. Phys. Soc. Jpn.* **21**, 631 (1966).

¹⁴R. O. Dillon, I. L. Spain, and J. W. McClure, *J. Phys. Chem. Solids* **39**, 1071 (1978).